2021

Dynamic Modeling of a Coal Mill for Simultaneous Dynamic Data Reconciliation and Parameter Estimation

vinayak dwivedy
West Virginia University, vd0025@mix.wvu.edu

Dynamic Modeling of a Coal Mill for Simultaneous Dynamic Data Reconciliation and Parameter Estimation

Vinayak Dwivedy

Thesis. submitted
to the Benjamin M. Statler College of Engineering and Mineral Resources
at West Virginia University

in partial fulfillment of the requirements for the degree of

Master of Sciences in Chemical Engineering

Debangsu Bhattacharyya, Ph.D., Chair
Nagasree Garapati, Ph.D.
Stephen Zitney, Ph.D.

Department of Chemical and Biomedical Engineering
Morgantown, West Virginia

2021

Keywords: Dynamic modeling, Coal Mill, VSM, Dynamic Data Reconciliation

Abstract

Dynamic Modeling of a Coal Mill for Simultaneous Dynamic Data Reconciliation and Parameter Estimation

Vinayak Dwivedy

In comparison with other gaseous and liquid fossil fuels used in power production, a coal fired power plants requires additional equipment for fuel preparation. A medium speed mill is usually a preferred equipment which serves in grinding and drying of the raw feed coal. Due to the high recycle of coal particles within a medium speed coal mill, the mill performance is sensitive to the efficiency of grinding and classification operations within mill. The goal of this research is to study the performance of the milling system and develop a method to estimate some of the unmeasured variables, which include pulverized fuel flow, fuel fineness, and mass of coal accumulated within mill.

In this work, a dynamic model of Vertical Spindle Mill (VSM) is developed using empirical formulations of size- reduction, and classification. While mass and energy balances are used to simulate moisture evaporation from coal particles. With the model developed in Aspen Custom Modeler, a simultaneous data reconciliation and parameter estimation experiment is setup for validating mill model using the measurements obtained from Industrial Partner Plant (IPP). The model is then used to study the performance of the mills operated in parallel, where the performance measure is obtained by calibrating and then comparing the efficiency parameters related to particle separation and grinding.

ACKNOWLEDGEMENTS

I would like to take this opportunity to thank Dr. Debangsu Bhattacharyya for presenting me with an opportunity to pursue my MS. under his guidance. His knowledge in the subject and support in setting up the reconciliation experiment helped me during the thesis. I would also like to thank Dr. Stephen Zitney, and Dr. Nagasree Garapati for being in my committee and providing their support and guidance. I would extend my thanks to Dr. Zitney for his knowledge on the subject by sharing the ongoing research work in the current field and sharing the industrial data, which was essential in the study. Finally, Dr. Garapati for our discussions during the course work classes.

I would like to extend my gratitude to National Energy Technology Laboratory through DE-FE0025912 contract for site support services and financial support. I would also like to also thank the Longview industrial partner plant for sharing their operational data.

My education and hard work would not be possible without the endless love and support of my parents and sister. Lastly, I would like to thank my fellow graduate students for all their insights and assistance in making this accomplishment.

Table of Contents

List of Figures

List of Tables

List of Abbreviations

N_{roll}	Number of rollers
$d_{i,avg}$	Diameter of 'i' th size coal (Average particle size on sieve size group 'i')
hg_{coal}, hg_{ref}	HGI index; Coal Feed and Reference respectively
η_a	Molecular velocity of air
B_{ij}	Breakage function
$C_1,\ C_2,\ C_3$	Classifier separation function constants
C_e	Adjustable constant in air velocity calculation
D_c	Diameter (Classifier)
D_{mt}	Diameter (Mill body)
M_{ic}	Mass accumulated of 'i' th size coal
N_{roll}	Number of rollers
$P_M, P_{no\ load}$	Power consumption; total and no-load respectively
R_u	Rosin Rammler parameter
S_{1i}, S_{2i}	Separation function; separator and classifier respectively
b_{ij}	Breakage matrix
d_{50}^s, d_{50}^c	Cut Diameter in Separator and Classifier zones respectively
k_a	Pressure drop Coeff.
k_{ac}	Pressure drop Coeff.
k_{en}	Pressure drop Coeff.
$\dot{m}$	Mass flow rate, Kg/s
u_{50}	Average velocity of air in the annular region above the grinding table
u_t	Characteristic tangential velocity in classifier
ΔP_{mill}	Pressure differential across mill
α_i	Selection function
β_i	Fraction of moisture evaporated
ρ_a, ρ_c	Density of air and coal respectively
F	Force on rollers
$Fine$	Fineness in %, passing 75 μm
R	Radius of contact point of rollers with grinding table
T	Temperature

x	Moisture accumulated in coal
τ	Residence time
ω	Angular velocity of grinding table
A_m	Mill metal area
h_{me}, h_{am}	Heat transfer coefficient

CHAPTER 1. INTRODUCTION

1.1 BACKGROUND

With the increasing use of renewable energy sources and their inherent variability in power generation, the load fluctuations in the power grid can be balanced by achieving faster ramp rates in a plant powered by fossil fuel. Compared to power production by fuels such as oil, natural gas, or nuclear energy, power production from coal has lower ramp rates. However, with advanced control strategies for fuel control, performance close to oil-fired power plants can be achieved (Rees, 1997). In a Supercritical Pulverized Coal (SCPC), coal is sent through the pulverizers, thereby increasing the surface area for combustion and liberation of volatile matter. As the fines impact flame stability, combustion efficiency, and NO_x generation (Curtis, 2005), at least 70% of the coal needs to be finer than 75 µm and 99.5% of the coal needs to be finer than 300 µm (Shi & Zuo, 2014). Additionally, due to the occurrence of mill faults and unmeasured internal states, the mill operation often limits the maximum ramp rates that coal-fired power plants can achieve.

Based on their speed, coal mills are classified into three types - low, medium, and high-speed mills. Due to their lower power consumption, a medium speed mill is most popularly used for pulverized fuel production (Shi et al., 2015).In this study, a vertical Spindle Mill (VSM), a medium-speed mill, is modeled. In general, these mills comprise of four zones: bowl, grinder, separator, and classifier. The feed enters the bowl and then proceeds to the grinder. Ground coal then gets conveyed to the classifier by the primary air. While smaller particles get carried to the classifier, the larger particles fall back to the bowl for re-grinding.

The operation of a VSM involves strong coupling among multiple operational variables, and time delay. Although several instruments have been developed for online measurement of pulverized fuel flow and moisture content of coal, they require frequent calibration thereby limiting their usage in online operation (Agrawal et al., 2015a). Furthermore, VSMs operate at high recycle loads (Shi et al., 2015). This internal circulation is highly sensitive to the grinding and classification efficiency, thereby affecting the performance as well as dynamics of the systems including slower ramp rates. As it is impractical to measure the internal circulation rates, mathematical models can be helpful for simulating the transient performance of the coal mills.

In a SCPC, a series of coal mills are operated in parallel to meet the energy requirement in the boiler. Although these mills are designed for same capacities, the performance of an individual mill is dependent on its health. While several dynamic mathematical models of a coal mill have been presented in the literature, there has been no study on validating models of multiple mills under load following conditions using the industrial data. The model can then be utilized for improving the mill performance under load-following operation.

One difficulty in validating the pulverizer model is the complicated interaction of several variables and lack of available measurements for some of the key variables. For example, the mill exit temperature depends on the flowrate and temperature of the primary air, amount of coal in recycle, and fed moisture content. With these motivations, this research is focused on developing a dynamic model of a coal pulverizer for proving an estimate of some of the unmeasured variables and monitoring the performance of an individual mill.

One difficulty in validating the pulverizer model is the complicated interaction of several variables. For example, the mill exit temperature depends on the flowrate and temperature of the primary air, amount of coal in recycle, and feed moisture content. In addition, the mill model includes several parameters that can greatly vary depending on the make and model of the mill and from mill to mill even for the same make and model depending on the operating and maintenance history of a mill. Therefore, model parameters need to be estimated. For parameter estimation (PE) using the industrial data, one difficulty is the lack of available measurements for some of the key variables such as the internal circulation rate within the mills, particle size distributions (PSD) from a mill, etc. Furthermore, industrial data often result in mass and energy balance errors and therefore data should be reconciled. If parameter estimation is performed using unreconciled data, estimated parameters can be biased. Therefore, it is desired that the data be reconciled for being used in estimation of model parameters. With these motivations, this research is focused on: (a) developing a dynamic model of a coal pulverizer for proving an estimate of some of the unmeasured variables, (b) reconcile the industrial data, (c) use the reconciled data for estimating model parameters.

In this work, the grinding model is based on the population balance for a given number of particle size distributions, while the classification model is based on the Rosin-Rammler efficiency curve. Even though the dynamic model is developed such that it is computationally tractable for dynamic optimization, solution of the dynamic optimization problem can be computationally intensive if the data from the industrial partner plant (IPP) available at each sampling instant is reconciled since it will lead to large number of decision variables. One key uncertain variable for mills is the air flowrate. If the air flowrate is reconciled at every couple of seconds and data over couple of hours are used for reconciliation, number of optimization variables can be very large. In the approach developed in this work, a model for the measurement error is proposed. Then the parameters of that error model are estimated along with process model parameters. This approach reduces the number of optimization variables by several orders of magnitude leading to a tractable dynamic optimization problem. Mill models involve many parameters. This can also lead to an increased size of the optimization problem and computational difficulty in software like Aspen. Therefore, a sensitivity-based approach is employed to down select the parameter space to be explored during parameter estimation.

Thus, in this work an approach is developed for simultaneous dynamic data reconciliation and parameter estimation using the data from the IPP. First a dynamic model of the mill is developed considering the key physical processes including coal comminution, moisture evaporation and classification. An empirical model is considered for particle breakage. The classification sub-model is developed using a separation function for computing the internal recycle of the oversized coal particles and the amount of moisture evaporated is computed from the overall energy balance.

CHAPTER 2. LITERATURE REVIEW

In a VSM, the coal feed enters the bowl and goes to the grinding table. Due to the rotating grinding table, the coal particles are pushed radially outwards and get crushed by the stationary rollers. The primary air that enters around the periphery of grinding table conveys the crushed particles to the classifier. Larger size particles cannot be conveyed to the classifier. They fall back to the bowl and are sent to the grinder along with the fresh feed. Oversized particles from the classifier returns to the bowl for regrinding, while the fines of desired size distribution go to the boiler for combustion. The hot primary air not only conveys the coal particles but also helps to evaporate the moisture from coal.

Mill operation requires careful control of the primary air flowrate and its temperature. A simplified process flow diagram of a typical fuel generation section in a SCPC power plant is presented in Figure 1. The primary air flowrate is varied to maintain the desired air to fuel ratio with due consideration of the classification efficiency. For controlling the mill outlet temperature, the inlet temperature of the primary air is regulated by manipulating the ratio of the hot air from the air preheater and a cold air stream that bypasses the air preheater, known as the tempered air. A lower temperature than desired can lead to incomplete evaporation of moisture from the coal while on the other hand, higher temperature than desired can lead to fire hazards. For uninterrupted operation of the mill, it is desired to get an estimate of the coal grindability and mass of coal accumulated in the mill. However, it is difficult, if not impractical, to measure both these variables real time. Therefore, typically, the power consumption at a given coal feed flowrate is used as a measure of the grindability of coal and the pressure difference across the mill is used as a measure of mass of coal accumulated in the mill (Agrawal et al., 2015b).

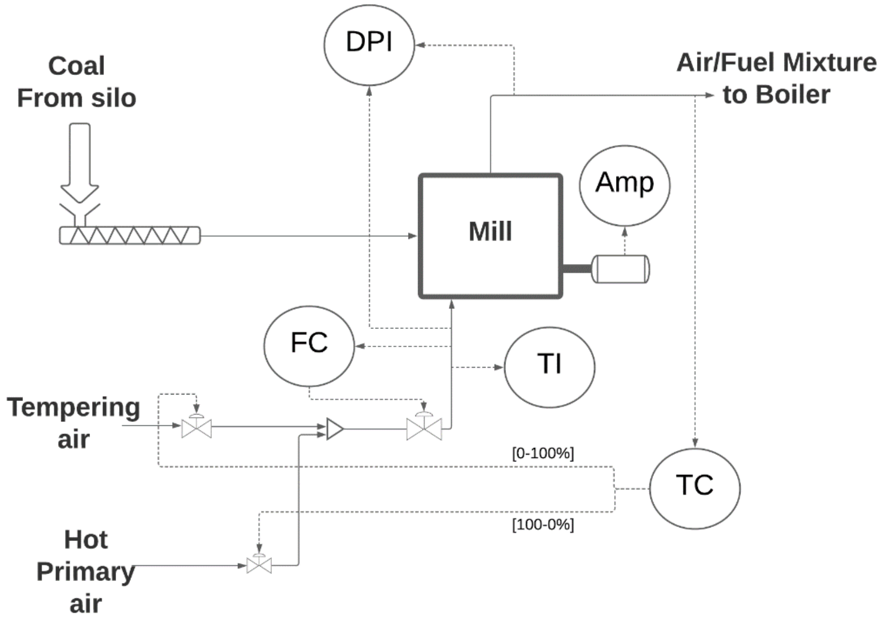

Figure 1: Simplified process flow diagram of milling section in a SCPC power-plant with indications of various measurements. (TC: Temperature controller, FC: Flow controller, TI: Temperature indicator, DPI: Pressure drop indicator, and Amp: Motor Current)

Several dynamic models for the coal mill have been communicated in the open literature. These models have been classified into detailed (Bhambare et al., 2010; Kojovic et al., 2015; Lee, 1986; Whiten & Özer, 2015) and simplified models (Agrawal et al., 2015a; Cortinovis et al., 2013; Gao et al., 2017; Niemczyk et al., 2012; Zhou et al., 2000).

The detailed model developed by Bhambare et al., are computational fluid dynamics (CFD) models that can provide high resolution of the spatial variation in the classifier and separator zones. The detailed dynamic model developed by Lee (Lee, 1986) divided the space from grinding table to classifier into 24 sectors while dividing the classifier cross sectional area into many small sections where force balance was applied to model pneumatic conveying of coal particles. These models are computationally expensive especially when the performance of multiple mills that operate in parallel are to be considered for plant-wide operation. Furthermore, detailed models require many parameters related to the mechanical details of the mill that are not necessarily available for commercial pulverizers due to proprietary reasons.

On the other hand, the simplified models can be used in real time applications such as mill control and can be used for estimating unmeasured variables such as the coal moisture content. Various simplified formulations presented (Niemczyk et al., 2012; Cortinovis et al., 2013; Gao et al., 2017) have shown a good agreement of model predictions for mill exit temperature, pressure drop and power consumption by validating the mill model using industrial data. The coal particles were discretized as either pulverized or unpulverized, and the grinding rate is expressed as a parameter while the classification rate is considered a time varying parameter. In order to capture the non-linearity at various mill loads, a multi-segmental approach for updating model parameters was proposed by Wei et al; (wei et al., 2007) and an improved accuracy over startup to shutdown operation were reported.

As the fineness of fuel plays a major role in combustion characteristics of pulverized coal, the size reduction due to breakage needs to be estimated. Earliest method for describing a breakage process was developed by Epstein (1948), where a probabilistic model considering a breakage function and probability of breakage, named as the selection function, were proposed. The selection function was used to describe the probability that a particle in a certain size would undergo breakage, while the breakage function was used to calculate the distribution of particle sizes generated after the breakage of a given particle size. Using the breakage and selection functions, (Broadbent & Callcott, 1956) introduced the matrix method for analyzing the breakage mechanism in various types of coal mills. Using modified selection and breakage functions, (Sligar, 1975) applied this matrix method to analyze size reduction in a continuous operating coal mill where the authors collected samples from the grinding table for comparison with the model. A similar form of selection and breakage functions were adopted by (Agrawal et al., 2015a; Lee, 1986; Zhou et al., 2000) for describing particle breakage in a dynamic model of a coal pulverizer. (Agrawal et al., 2015a; Zhou et al., 2000) presented a dynamic model of VSM, where the selection function was dependent on hardness and size of the particle. By analyzing the coal feed and pulverized fuel flows for particle size distributions during steady state operation, the fuel fineness from the work of (Agrawal et al., 2015a) was found to be in good agreement with the industrial data obtained from a VSM in a 500 MW coal fired power plant. Furthermore, a good fit for mill exit temperature, pressure drop, and power consumption were reported using a constant value of the model parameters.

The hardness of coal can be dependent on various factors such as mineral content, rank , age, and location within mine. The Hardgrove grindability index (HGI) is widely used as a measure of grindability of coal. It was noted in the work of (Shi & Zuo, 2014) that the power consumption during the testing time in a standard HGI testing equipment varies although the speed of grinder remains constant. Thus, an energy-based size reduction function was introduced where measured torque data from an additional sensor was used. Using this new function for predicting particle breakage, a steady state model of a VSM was developed by (Shi et al., 2015) by separating machine and material dependent parameters. However, this method required extensive sampling and testing of coal samples in the newly developed hardness testing machine.

It is observed from the literature review that there is hardly any work where uncertainties in measurement data have been considered during model validation. Furthermore, there are lack of industrial data used for model validation especially when the data are collected from multiple mills and the plant is undergoing load-following operation. Such data also exhibit mill to mill variabilities leading to a challenging problem for model validation. Furthermore, there is hardly any work in the literature where a dynamic optimization problem has been undertaken for dynamic data reconciliation and parameter estimation. With these motivations, the research objectives are as follows:

Objective 1: Development of the dynamic mill model

Objective 2: Dynamic data reconciliation and parameter estimation

CHAPTER 3. METHODOLOGY

3.1 DYNAMIC MODEL OF A VERTICAL SPINDLE ROLLER MILL

The objective of this task is to develop a dynamic model of a VSM with consideration of Particle Size Distribution in breakage and classification operation. Additionally, to calculate performance parameters for monitoring the mill operation. For modeling a VSM, the internal regions are divided into four regions: Bowl, Grinding, Separation and Classification zones, as depicted in Figure 2. A detailed description of model equations is presented in Appendix. With an aim to simplify the operation of the mill and application for model in online monitoring, following assumptions have been made:

1. The particle size is discretized into ten size groups as listed in Table. 1. The size distribution of feed is assumed constant and same for all mills.
2. Moisture is uniformly distributed among all particle sizes.
3. Effects of varying roller pressure and bypass in grinding section are not modeled. It is assumed that the extent of breakage of particles in a given size group remains unaffected irrespective of the concentration of that particle group in the feed to the grinding section.
4. The temperature of coal leaving the mill is assumed to be the same as the temperature of coal entering the classifier zone.

Table 1: Discretization of particle size based on sieve sizes (Agrawal et al., 2015a)

Size, i	ASTM Mesh Size/Number	Sieve opening (mm)	Average particle size (mm)
1	3/8"	9.5	14.25
2	4	4.75	7.125
3	8	2.36	3.555
4	16	1.18	1.77
5	30	0.6	0.89
6	50	0.3	0.45
7	100	0.15	0.225
8	200	0.075	0.1125
9	400	0.038	0.0565
10	625	0.02	0.029

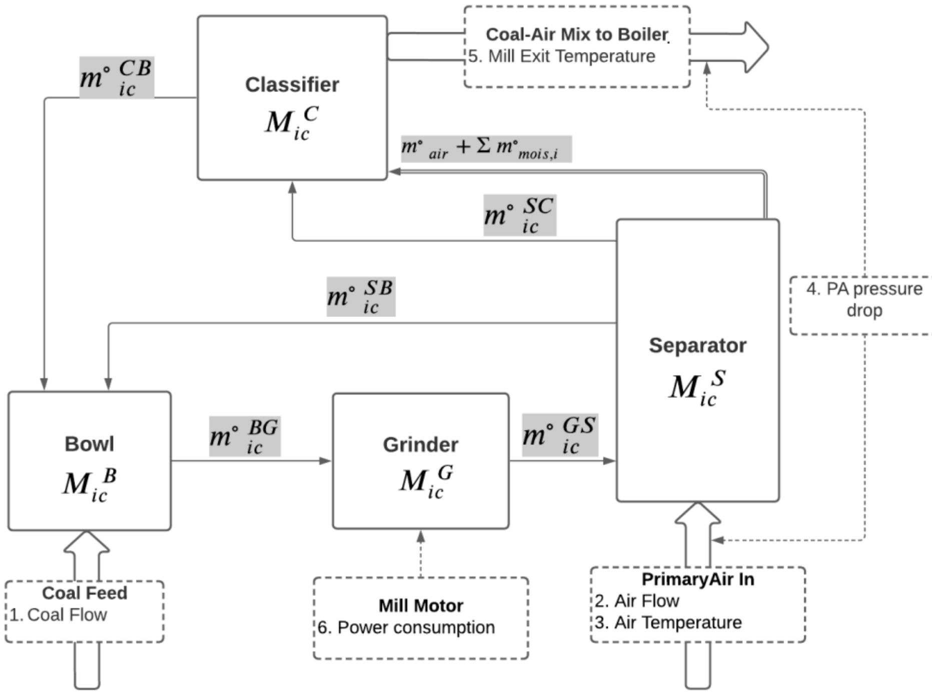

Figure 2: Schematic of modeling zones showing coal flows within each zone (highlighted) and measured variables (numbered) (Agrawal et al., 2015a)

The mass balance equations for the mill model are below. As a general representation of model variables in the conservation equations, the mass accumulated in any zone is represented by M_{ic} and the mass flow rate of coal from one zone to other is represented using '$\dot{m}_{ic}$'. For example, M_{ic}^{B} is the mass of ith size coal accumulated in bowl, and $\dot{m}_{ic}^{FB}$ is the mass flow of ith size coal from the feeder to the bowl. The size reduction in Grinding zone is represented by $\left(-\alpha_i M_{ic}^{G} + \sum_{j=1}^{i} b_{ij}\alpha_j M_{ic}^{G}\right)$, where α and b denote the selection and breakage matrix respectively.

$$\frac{dM_{ic}^{B}}{dt} = \dot{m}_{ic}^{FB} + \dot{m}_{ic}^{SB} + \dot{m}_{ic}^{CB} - \frac{M_{ic}^{B}}{\tau_{bg}} \tag{1}$$

$$\frac{dM_{ic}^{G}}{dt} = \dot{m}_{ic}^{BG} + \left(-\alpha_i M_{ic}^{G} + \sum_{j=1}^{i} b_{ij}\alpha_j M_{ic}^{G}\right) - \frac{M_{ic}^{G}}{\tau_{gs}} \tag{2}$$

$$\frac{dM_{ic}^{S}}{dt} = \dot{m}_{ic}^{GS} - S_{1i}\left(\frac{M_{ic}^{G}}{\tau_{sc}}\right) - (1 - S_{1i})\left(\frac{M_{ic}^{G}}{\tau_{sb}}\right) - \dot{m}_{mois,i} \tag{3}$$

$$\frac{dM_{ic}^{C}}{dt} = \dot{m}_{ic}^{SC} - \frac{M_{ic}^{C}(1 - S_{2i})}{\tau_{cb}} - \frac{M_{ic}^{C}(S_{2i})}{\tau_{cfu}} \tag{4}$$

The separation of particles in the Separator and Classifier zones is represented using the separation function, which is calculated using the Rosin-Rammler efficiency curve as given by Eq (5) and (6) respectively. The resulting model can represent both the passive (due to primary air lift) and active (due to centrifugal effects) particle size separation taking place in the mill.

$$S_{1i} = \exp\left(-0.6931\left(\frac{d_{i,avg}}{d_{50}^{s}}\right)^{\alpha_s}\right) \tag{5}$$

$$S_{2i} = \exp\left(-0.19\left(\frac{d_{i,avg}}{d_{50}^{c}}\right)^{\alpha_c}\right) \tag{6}$$

The cut diameter (d_{50}^{s}) passing from separator to classifier is calculated using a correlation for the drag force developed by (Whiten & Özer, 2015), where the terminal velocity of air in the annular region just below the classifier is approximated using an adjustable constant. While, for the classifier zone a constant Stoke's number is used for calculating the separation function. It should be noted that the efficiency of particle separation is calibrated using the efficiency parameters α_s and α_c.

In a CFD study conducted by (Bhambare et al., 2010), the temperature of air entering classifier zone was found to be almost equal to the mill exit temperature. In this study, it is assumed that moisture evaporation only occurs in the separator zone. The energy balance equations are presented by Eq (7), (8), and (9). Where Eq (7) represents the combined energy balance for the bowl and grinding zones. The energy balance for the separator zone is presented in Eq (8) and (9), where the heat released from air aids in raising the temperature of coal, moisture evaporation from coal, and heat loss from mill metal to environment.

$$cp_c \frac{d}{dt}\left(T_g \sum (M_{ic}^{B} + M_{ic}^{G})\right) = cp_c\, T_f \dot{m}_{ic}^{FB} + cp_c\, T_{out}\dot{m}_{ic}^{CB} + cp_c\, T_{out}\dot{m}_{ic}^{SB} - cp_c\, T_g \dot{m}_{ic}^{GS} + Q_g \tag{7}$$

$$\dot{m}_{air} cp_a \left(T_{a,in} - T_{out}\right) = cp_c \left(T_{out} - T_g\right) \sum \left(\dot{m}_{ic}^{SC} + \dot{m}_{ic}^{SB}\right) + h_v \sum \dot{m}_{mois,i} + h_{am}\left(T_{avg} - T_m\right) \tag{8}$$

$$M_m cp_m \frac{d}{dt}(T_m) = h_{am}\left(T_{avg} - T_m\right) - h_{me} A_m (T_m - T_{amb}) \tag{9}$$

(Shi & Zuo, 2014) observed that the power required in a HGI testing equipment was dependent on the initial size and relative density of the test sample. However, due to continuous operation in a VSM as opposed to batch testing in a HGI equipment, a same power consumption formulations cannot be used for the two different types of grinding equipment. By sampling the mill internal samples and analyzing the PSD a power consumption model was developed by (Shi et al., 2015), where it was noted that an increase in the fines accumulation within the mill can lead to increased power consumption which can be accounted to the mineral matter: being more abrasive than combustible coal. In this study, the power consumption is given by Eq. (10), where the total power consumption is calculated by summing the power required to run an empty mill and the power required to pulverize the coal in the grinding zone. The frictional coefficient between the rollers and rotating table (μ**)** is related to the mass of total coal accumulated and the amount of fines in grinding zone, as given by Eq. (11).

$$P_M = \mu\, F\, R\, \omega\, N_{roll} + P_{no\ load} \tag{10}$$

$$\mu = C_1 \left\{ 1 - exp\left(- \frac{\sum_{i=1}^{10} M_{ic}^G}{C_2} \left(\frac{\sum_{i=8}^{10} M_{ic}^G}{\sum_{i=1}^{10} M_{ic}^G} \right)^{C_3} \right) \right\} \tag{11}$$

$$I = \frac{P_M}{V\, P_f} \tag{12}$$

The pressure differential across the mill is calculated by using Eq. (13) similar to (Agrawal et al., 2015a), which relates pressure drop due to three conditions. Firstly, due to mass flow rate of air, secondly due to mass of coal accumulated on grinding table and lastly due to amount of coal in suspension in separator and classifier zones.

$$\Delta P_{mill} = k_a \dot{m}_a^2 + k_{ac} \dot{m}_a^2 \sum_{i=1}^{10} (M_{ic}^G + M_{ic}^B) + k_{en} \dot{m}_a \sum_{i=1}^{10} (M_{ic}^S + M_{ic}^C) \tag{13}$$

3.2 SENSITIVITY ANALYSIS

A study is undertaken to evaluate the sensitivity of measured variables with respect to the model parameters. This approach can help to downselect the parameter space to be explored for parameter estimation thus reducing the size of the optimization problem. For conducting sensitivity analysis, a derivative based local method is used to select parameters before the estimation run (Morgan et al., 2015). A base case was generated using the referenced value of model parameters. The first step in parameter sensitivity analysis involves the calculation of sensitivity matrix, as presented in Eq.(14), where y, u, and θ indicate output variables, input variables and parameters, respectively. Next, a normalized sensitivity value is calculated using Eq. (15), which scales the parameter sensitivity between one and zero. The parameter sensitivity study was conducted by varying the parameters by 20% of their referenced values. The normalized sensitivity values for the model parameters are presented in Table 2, where the values along the rows indicate the normalized sensitivity of a model parameter with respect to the respective model outputs.

$$\mathrm{S_{ij}} = \max_{\mathrm{u_j} \in \left[\mathrm{u_j^L}, \mathrm{u_j^U}\right]} \left| \frac{\partial \mathrm{y}}{\partial \Theta_\mathrm{i}} \right|_{\mathrm{u_j}} \tag{14}$$

$$\mathrm{N_{ij}} = \frac{\mathrm{S_{ij}}}{\max\,(\mathrm{S_{ij}})} \tag{15}$$

Table 2: Normalized sensitivity values for model parameters

Parameter	Description	ΔP_{mill}	P_M	T_{out}
τ_{bg}	Zone residence time	0.316	0	0
τ_{gs}	Zone residence time	0.013	0.094	0.019
τ_{sc}	Zone residence time	0.077	0.022	0.003
τ_{sb}	Zone residence time	0.054	0.021	0.003
τ_{cf}	Zone residence time	0.174	0.051	0.008
τ_{cb}	Zone residence time	0.145	0.051	0.007
K_s	Grinding rate	0.346	0.128	0.018
α_s	Separator efficiency	0.089	0.031	0.004
h_{me}	Heat transfer coeff.	0	0	0
h_{am}	Heat transfer coeff.	0	0	0
α_c	Classifier efficiency	0.33	0.096	0.014
k_a	Pr. drop parameter	0.389	0	0
k_{ac}	Pr. drop parameter	0.712	0	0
k_{en}	Pr. drop parameter	0.03	0	0
x^F	Feed moisture content	0.051	0.017	0.945
C_2	Motor current parameter	0	0.246	0
C_3	Motor current parameter	0	0.184	0
F	Roller pressure	0	1	0.001

3.3 SIMULATENEOUS DATA RECONCILIATION AND PARAMETER ESTIMATION

Industrial data may have gross and random errors and often fails to satisfy material and energy balances thus requiring data reconciliation (Narasimhan, 1999). If these data are used for data reconciliation, then the estimated parameters can be biased. As the dynamic data from the IPP will be used, data reconciliation involves solving a dynamic optimization problem. As certain parameters used in the mill model are used as an indication of mill performance, it is desired to solve a PE problem as well. DDR and PE problems can be solved as a two-stage optimization problem for tractability, but that approach can suffer from optimality gap and excessive iteration, additionally it is not feasible for an equation-oriented platform like ACM. Therefore, in this work, the following Least squared problem will be solved for DDR and PE using the Estimation tool in ACM:

$$\min\ \left(y_{exp}-y\right)^T \sum\nolimits^{-1} \left(y_{exp}-y\right)$$
$$\text{Subjected to:} \tag{16}$$
$$f(x,\dot{x},y,u,\theta)=0$$
$$g(x,y,u,\theta)\leq 0$$

In Eq. (16), x, y, u, θ indicate differential variables, algebraic variables, input variables and parameters, respectively. The mill model described before is a differential algebraic equation system. In Eq. (17), $f(.)$ and $g(.)$ denote the differential and algebraic equations. Before performing the estimation run in ACM, a few pre-requisites are performed and involves the following steps:

Step 1: Pre-processing of the raw measurement data

The data from IPP is noisy. In this study, the Industrial data is sampled at every ten seconds and a Load-Following data set of Fifty-thousand seconds is used to study the mill performance. The data is sent through a centered moving average filter with a moving window interval of five minutes.

Step 2: Normalization of output variables

Scales of different measurements such as the air and coal flowrates versus pressure drop versus the power consumption and temperature vary widely. Units used also affect the scales. Thus, if the raw data with their given units are used, it can lead to biased estimate. Therefore, all data are normalized before being used in the DDR using the following equation:

$$y_{scaled}=\frac{y-y_{min}}{y_{max}-y_{min}} \tag{17}$$

Where, y represents the measurement variable and a separate minimum and maximum limit for each measurement variable is used in the formulation above.

Step 3: DDR and PE

As the measurement data available from the IPP are sampled every 10 sec, it will lead to large number of decision variables. For example, if one considers 2-hour worth of data, it will lead to 720 decision variables for a single measurement variable that needs to be reconciled. If the length of the data is increased and/or frequency of sampling is increased, the number of decision variables will linearly grow leading to computational intractability especially in the ACM optimization environment. Therefore, a measurement error model is used for reconciling the measured variables. Considering a linear error model, then:

$$\begin{gathered} y_{reconciled} = a\, y_{exp} + b \\ a = h(y_{exp}) \\ b = m(y_{exp}) \end{gathered} \tag{18}$$

Measurement model parameters, *a* and *b*, are considered as a function of the experimental data. It should be noted that during the single ramp down study using Industrial data, the error model for a single measured variable lead to only 4 decision variables if the error model and the model for *a* and *b* are linear. In addition, the number of decision variables does not change with the change in the sampling frequency and length of the data.

CHAPTER 4. RESULTS AND DISCUSSIONS

4.1 MODEL VALIDATION AND RECONCILIATION RESULTS

In this study, the PSD of coal feed and the breakage model were referenced from the work by (Agrawal et al., 2015a). Since the sampling results from IPP were not available, the results for PSD of pulverized fuel were compared with the requirements listed by (Curtis, 2005); such that at least 70% of the coal needs to be finer than 75 µm and 99.5% of the coal needs to be finer than 300 µm. However, a lab analysis for moisture fraction of raw feed was used from IPP data. A logarithmic cumulative size distribution representing the fraction of flow passing the specified sieve opening are presented in Figure 3.

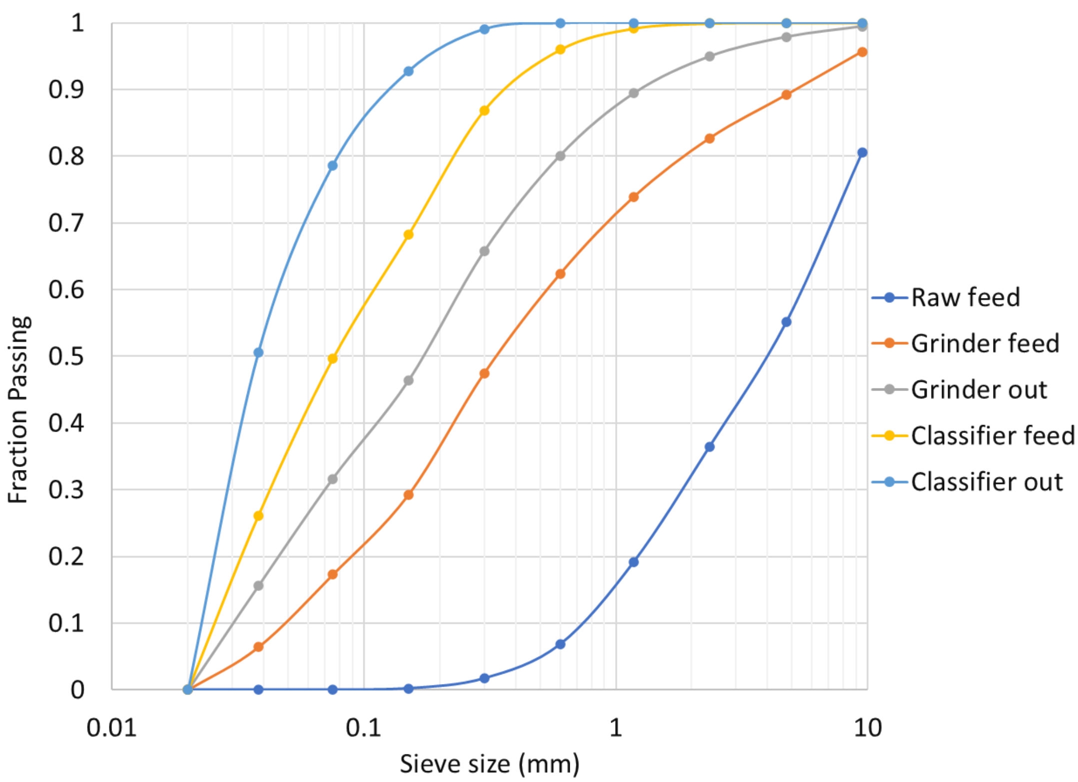

Figure 3: Cumulative size distribution representing fraction passing the specified size for various streams within mill

With the parameters selected from sensitivity analysis, a simultaneous DDR and PE experiment was conducted. The industrial data from three mills operating in parallel was used to analyze the performance of mill(s). Model parameters estimated during this experiment are listed in Table 3.

Table 3: Estimated Model Parameters

Parameter	Description	Mill #1	Mill #2	Mill #3
τ_{bg}	Bowl residence time (sec)	22.79	17.68	7.00
α_c	Classifier efficiency	0.88	0.72	0.68
α_s	Separator efficiency	0.656	0.771	0.97
K_s	Grinding rate	0.36	0.52	0.602
C_1	Frictional Coeff.	0.147	0.147	0.159

An increase in the grinding rate results in a decrease in the coal bed height in bowl zone and an increase in power consumption. It can be seen from the estimated parameters that where the mill has a higher grinding rate, it has lower residence time in the bowl zone. Additionally, it is observed that a decrease in the separator efficiency leads to increased mass accumulation within the mill.

In this study, only the air flow to the mill is reconciled. It should be noted that the mill exit temperature is controlled at a desired setpoint by a control system. Figures 4, 5, and 6 show the plots for measured and predicted values of measured variables for the three mills respectively. The plots are generated using the scaled values of the variables due to the proprietary industrial data. It can be observed in these results that the motor current has large variability. Possible reasons for the variability are the non-uniform distribution of the particle sizes on the grinding table and non-uniformity in their hardness.

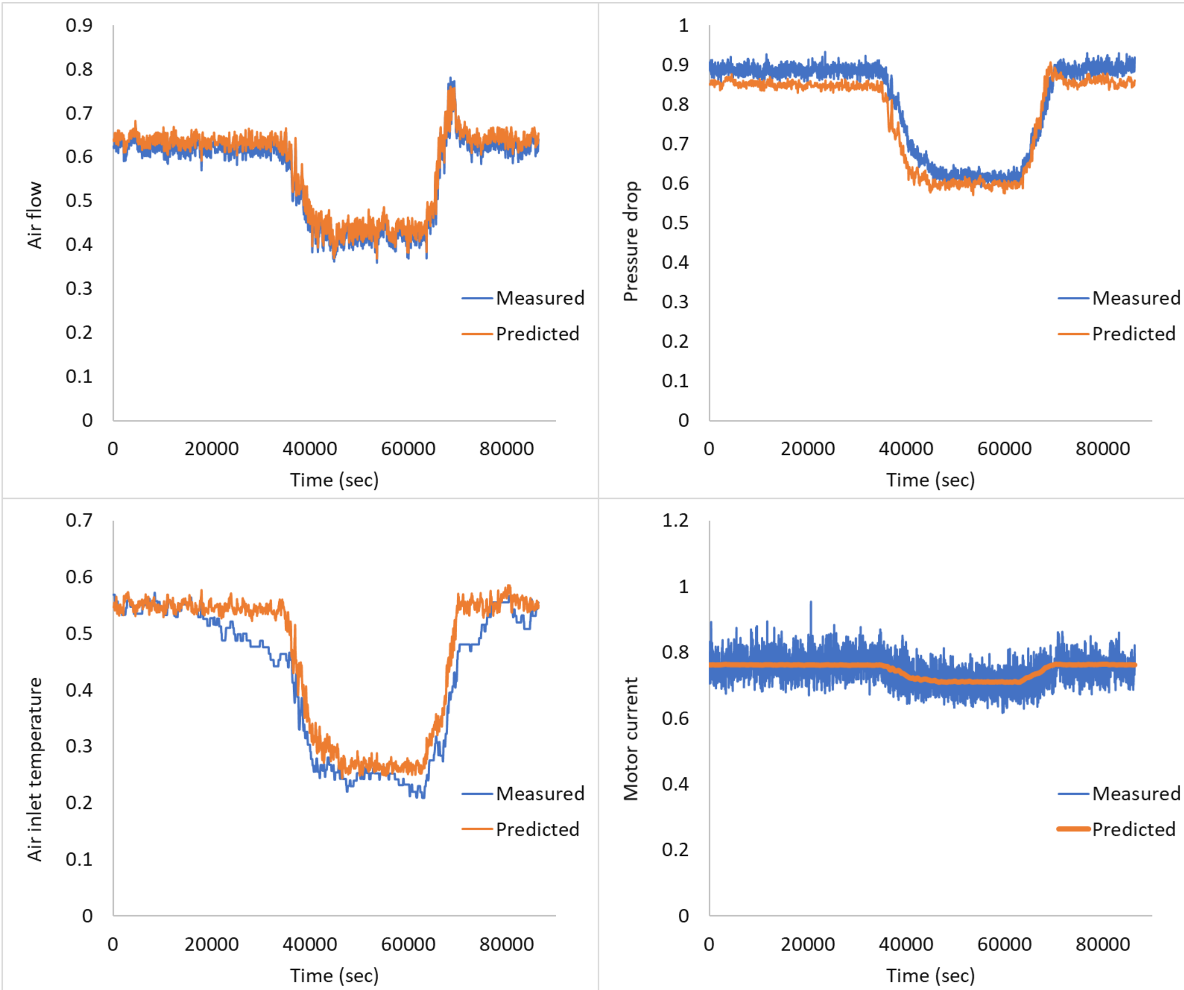

Figure 4: Comparison of Measured and predicted values of measured variables for Mill #1

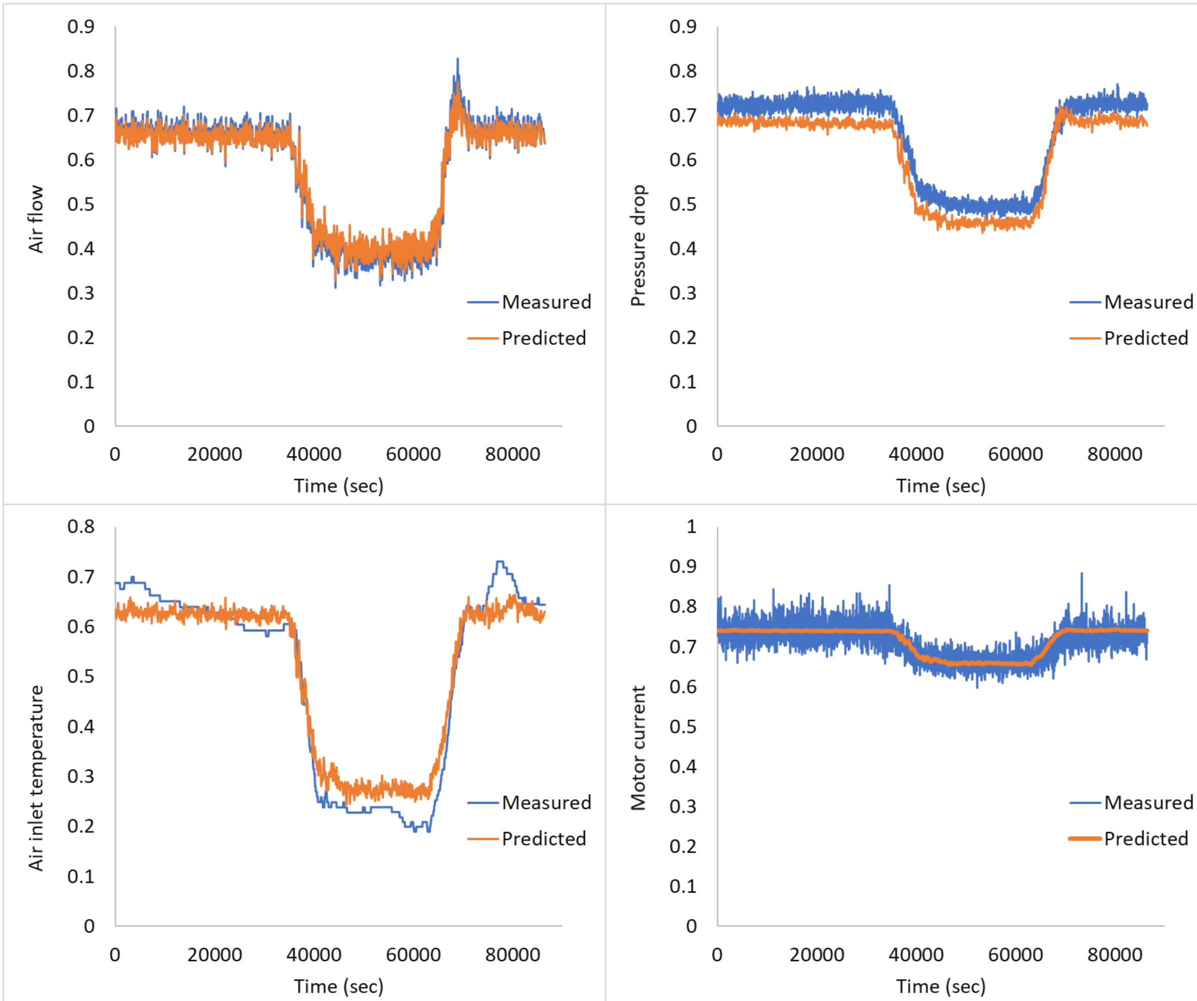

Figure 5: Comparison of Measured and predicted values of measured variables for Mill #2

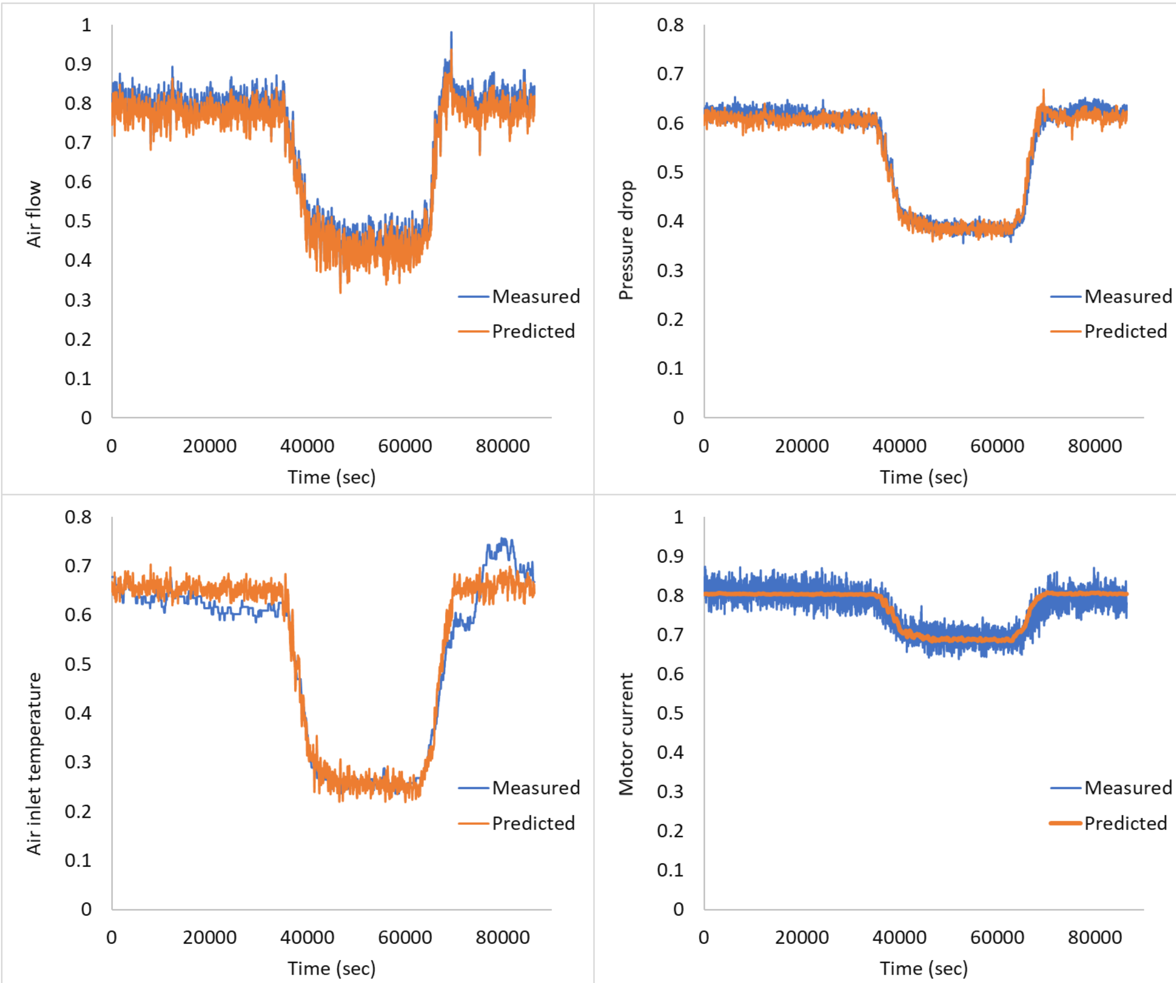

Figure 6: Comparison of Measured and predicted values of measured variables for Mill #3

One of the problems in the mill operation is saturation, where the increased mass accumulation of coal can lead to increased pressure drop and eventually clogging of the mill. For this reason, the recycle ratio is calculated as a performance measure of the mill as presented in Eq. (19), which is defined as the coal mass flow out of grinding zone divided by the total raw feed coal mass flow. This definition is somewhat different than recycle ratio definitions used in conventional chemical engineering problems, but is typically used for pulverizers. The product fineness is defined as the fraction of coal passing the screen with an opening of 75 μm, which in this study represents the size fraction $i = 8$ and calculated using Eqn. (20).

$$Recycle = \frac{\sum(\dot{m}_{ic}^{GS})}{\sum(\dot{m}_{ic}^{FB})} \tag{19}$$

$$\text{Fine} = \frac{\sum_{i=9}^{10} \dot{m}_{ic}^{CFu}}{\sum_{i=1}^{10} \dot{m}_{ic}^{CFu}} \tag{20}$$

4.2 FAULT SIMULATION

The fuel preparation section in a coal fired power plant is susceptible to occurrence of faults with a majority of problem related to solids handling. Although a few fault detection simulations are available in open literature (Guo et al., 2014; Hu et al., 2020), there is a lack of a study which considers a detailed particle discretization for coal particles. In this section, a few fault simulations are conducted to provide an insight in the operation of the mill during the occurrence of faults which can be useful in developing a trigger alarm incase these faults are detected.

The fault simulations are conducted by ramping the respective performance parameter related to the fault. A steady state operation of the mill is simulated for 100 seconds and the ramping of parameter is performed in 60 seconds. Additionally, the same control strategy during model validation is used; where a constant air inlet flow and mill exit temperature are maintained while manipulating the tempering air flow. In this study, the following faults are discussed: feeder tube choking, decreased grinding rate, decreased separator efficiency.

FEEDER TUBE CHOKING

As the coal is transferred from storage silos to the mill, the large sized particles of coal can cause choking of coal in feeder tube. Thereby resulting in a decreased or total stoppage of coal to the mill. This fault is simulated by decreasing the coal flow from 35,544 kg/hr to 17,772 kg/hr and an effect on the other measured and performance variables is presented in Figure 7. A gradual decrease in coal mass accumulation in bowl and grinding zones is observed. The major safety concern during this fault is to maintain the air inlet temperature as a failure to do so could lead to mill fire due to the contact of high temperature air with a decreased mass of coal in mill.

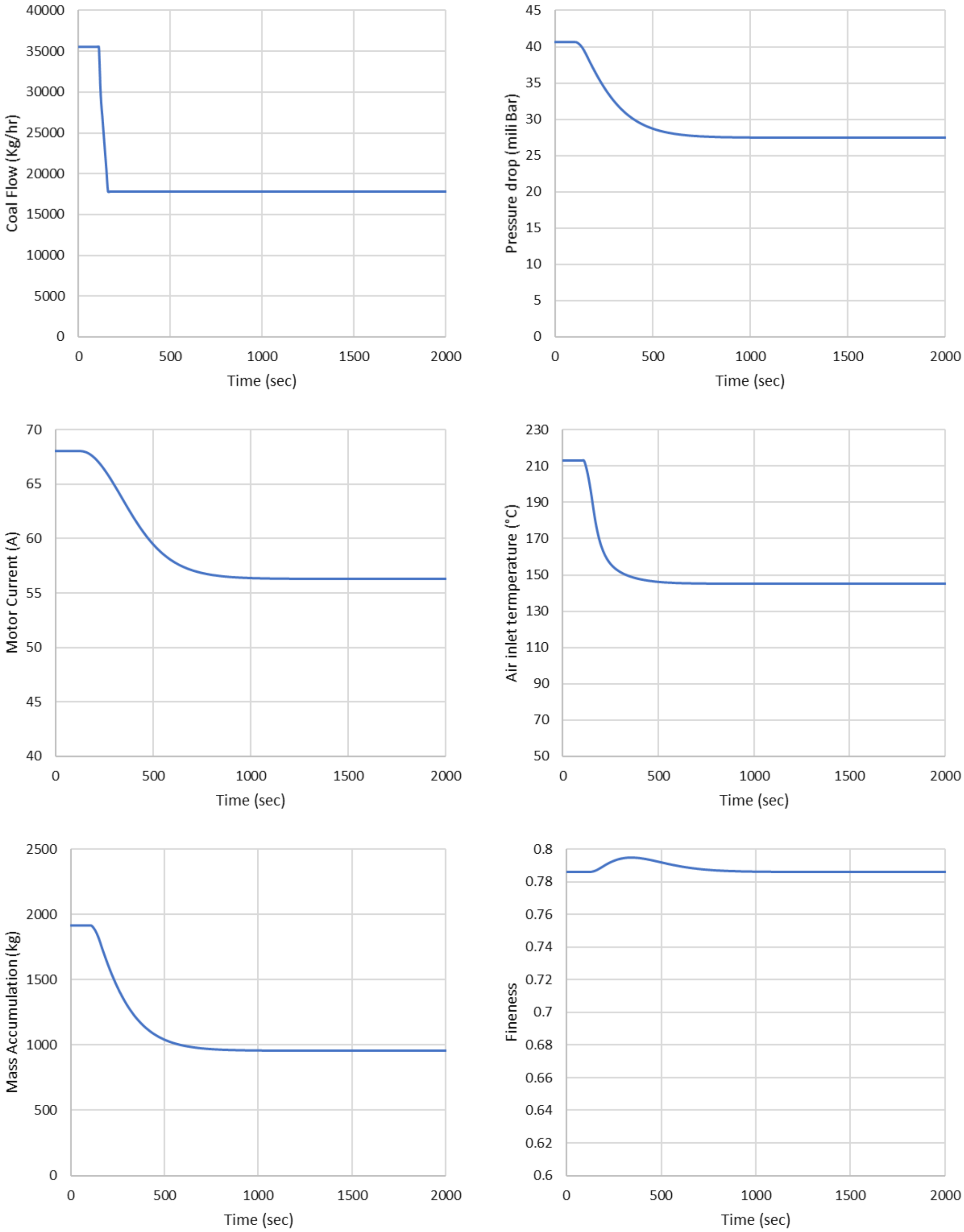

Figure 7: Simulation of feeder tube choking

DECREASED GRINDING RATE

With the continuous operation of a coal mill, grinding rate of a mill would deteriorate with time. Figure 8 shows the effect of decreasing the grinding rate parameter (K_s) from 0.52 to 0.26. It should be noted that the grinding rate parameter is expected to change over months as opposed to seconds as has been simulated in this work. This is done merely to study the impact on the key output variables. From that perspective, the dynamics of the output variables shown in Figure 8 are not meaningful, but the corresponding steady-state values of those variables are. In this simulation, it can be seen from the plots that due to the occurrence of the fault, the mass accumulation of coal in the bowl and grinding zones combined increases due to the decreased grinding rate. Additionally, the motor current decreases due to the decreased frictional coefficient between the rollers and grinding table, and later stabilizing at the same value when the amount of fines concentration within mill equalizes.

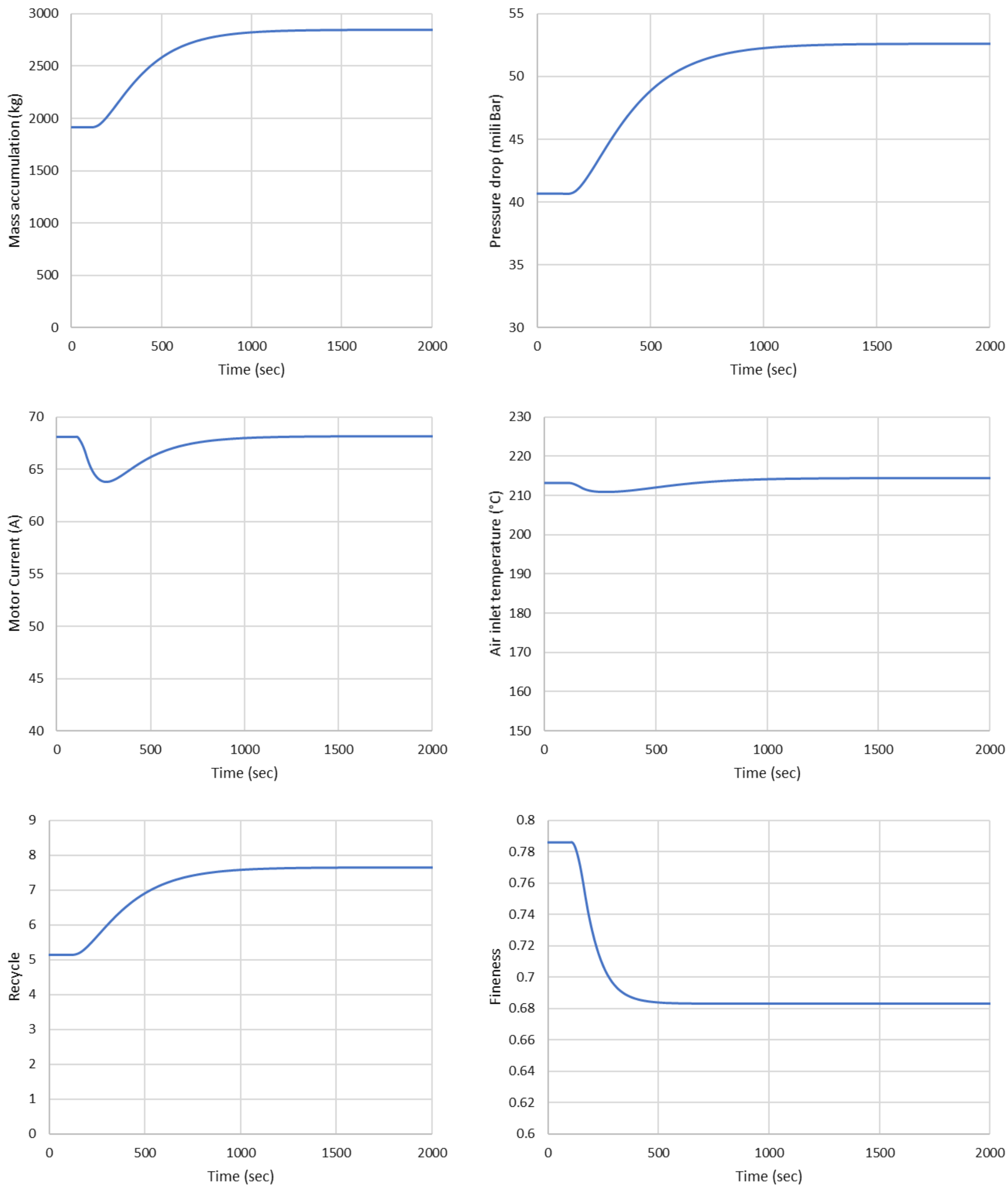

Figure 8: Simulation of decreased grinding rate

DECREASED SEPARATOR EFFICIENCY

One of the major faults in the operation of a VSM includes the blockage or damage to the air vanes surrounding the grinding table. Due to this fault, a non-uniform air velocity can occur in the annular region above the grinding zone thereby leading to an abnormal carryover of large particles to the classifier zone. Figure 9 shows the simulation of this fault and is performed by decreasing separator efficiency parameter (α_s) from 0.771 to 0.5. During this fault, an increase in the coal mass accumulation in the bowl and grinding zone is observed, which is also indicated by a final increase in the motor current after the fault.

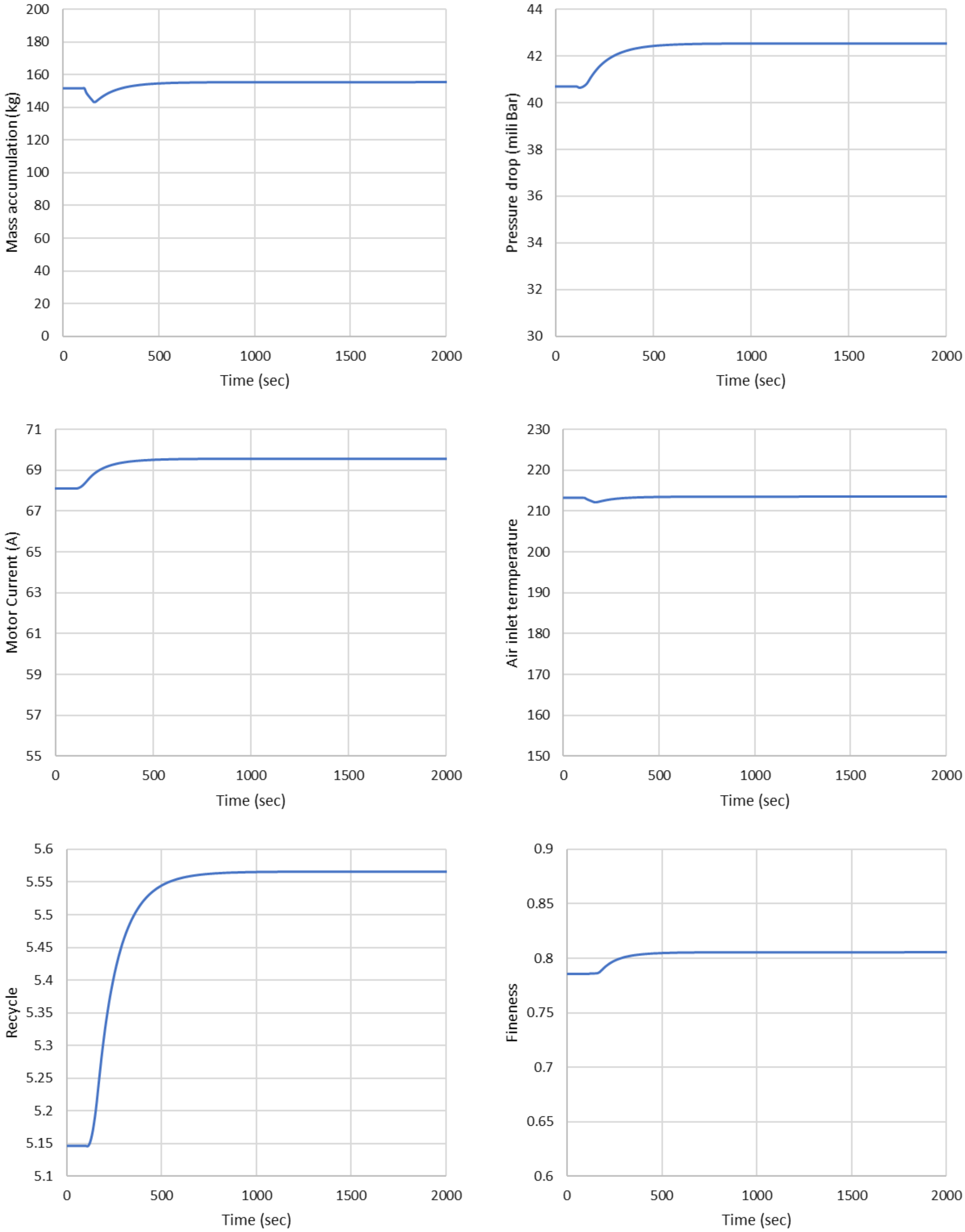

Figure 9: Simulation of decreased separator efficiency

CHAPTER 5. SUMMARY AND RECOMMENDATIONS

A dynamic model of a VSM was developed and validated using the industrial data. The resulting model can represent both the passive (due to primary air lift) and active (due to centrifugal effects) particle size separation taking place in the mill. Additionally, the coal particles are discretized in ten size groups and an empirical formulation for breakage model is considered in the study. As an application of the developed model, it can be used to monitor the online maintenance health of the mill components and developing strategies to improve the mill performance.

A few recommendations are presented to improve the estimation capabilities of the model and future works:

- In this study, only the air flow to the mill was reconciled, however for reconciling coal flow, the model needs to be integrated with the boiler model to accurately predict the heat duty requirement by the power plant.
- With a regular sampling and analysis of pulverized fuel and Raw feed for PSD, the model parameters can be again estimated to monitor the fineness specification of pulverized fuel.
- For the application of model in online monitoring and fault detection, additional measurements from vibrational sensors can be used to improve the reliability of mill control.

References

Agrawal, V., Panigrahi, B. K., & Subbarao, P. M. V. (2015). A unified thermo-mechanical model for coal mill operation. *Control Engineering Practice*, *44*, 157-171.

Agrawal, V., Panigrahi, B. K., & Subbarao, P. M. V. (2015). Review of control and fault diagnosis methods applied to coal mills. *Journal of Process Control*, *32*, 138-153.

Bhambare, K. S., Ma, Z., & Lu, P. (2010). CFD modeling of MPS coal mill with moisture evaporation. *Fuel processing technology*, *91*(5), 566-571.

Bhattacharya, C. (2008). Capacity mapping for optimum utilization of pulverizers for coal fired boilers. *Journal of Energy Resources Technology*, *130*(3).

Bollinger, K. E., & Snowden, H. R. (1983). The experimental determination of coal mill models. *IEEE Transactions on Power Apparatus and Systems*, (6), 1473-1477.

Broadbent, S. R., & Callcott, T. G. (1956). A matrix analysis of processes involving particle assemblies. *Philosophical Transactions of the Royal Society of London. Series A, Mathematical and Physical Sciences*, *249*(960), 99-123.

Cortinovis, A., Mercangoez, M., Mathur, T., Poland, J., & Blaumann, M. (2013). Nonlinear coal mill modeling and its application to model predictive control. *Control Engineering Practice*, *21*(3), 308-320.

Curtis, J. S. (2005). *Coal Particle Flow Patterns for O2 Enriched, Low NOx Burners*. Purdue Univ., West Lafayette, IN (United States).

Epstein, B. (1948). Logarithmico-normal distribution in breakage of solids. *Industrial & Engineering Chemistry*, *40*(12), 2289-2291.

Fakourian, S., Fry, A., & Jasperson, T. (2018). Analysis of particle behavior inside the classifier of a Raymond Bowl Mill while co-milling woody biomass with coal. *Fuel Processing Technology*, *182*, 95-103.

Guo, S., Wang, J., Wei, J., & Zachariades, P. (2014). A new model-based approach for power plant Tube-ball mill condition monitoring and fault detection. *Energy conversion and management*, *80*, 10-19.

Gao, Y., Zeng, D., & Liu, J. (2017). Modeling of a medium speed coal mill. *Powder Technology*, *318*, 214-223.

Hu, Y., Ping, B., Zeng, D., Niu, Y., & Gao, Y. (2020). Modeling of Coal Mill System Used for Fault Simulation. *Energies*, *13*(7), 1784.

Kojovic, T., Shi, F., & Brennan, M. (2015). Modelling of vertical spindle mills. Part 2: Integrated models for E-mill, MPS and CKP mills. *Fuel*, *143*, 602-611.

Lee, M. S. (1986). *Mathematical model and control of a coal pulverizer* (Doctoral dissertation, The University of Texas at Austin).

Leśniak, B., Słupik, Ł., & Jakubina, G. (2013). The determination of the specific heat capacity of coal based on literature data. *Chemik*, *67*(6), 560-571.

Morgan, J. C., Bhattacharyya, D., Tong, C., & Miller, D. C. (2015). Uncertainty quantification of property models: Methodology and its application to CO2-loaded aqueous MEA solutions. *AIChE Journal*, *61*(6), 1822-1839.

Narasimhan, S., & Jordache, C. (1999). *Data reconciliation and gross error detection: An intelligent use of process data*. Elsevier.

Niemczyk, P., Bendtsen, J. D., Ravn, A. P., Andersen, P., & Pedersen, T. S. (2012). Derivation and validation of a coal mill model for control. *Control Engineering Practice*, *20*(5), 519-530.

Özer, C. E., Whiten, W. J., & Lynch, A. J. (2016). A multi-component model for the vertical spindle mill. *International Journal of Mineral Processing*, *148*, 155-165.

Rees, N. W. (1997). Advanced power plant control for large load changes and disturbances. *IFAC Proceedings Volumes*, *30*(17), 601-608.

Shi, F., Kojovic, T., & Brennan, M. (2015). Modelling of vertical spindle mills. Part 1: Sub-models for comminution and classification. *Fuel*, *143*, 595-601.

Shi, F., & Zuo, W. (2014). Coal breakage characterisation–Part 1: breakage testing with the JKFBC. *Fuel*, *117*, 1148-1155.

Shoji, K., Meguri, N., Sato, K., Kanemoto, H., Hasegawa, T., & Maruyama, T. (1998). Breakage of coals in ring-roller mills Part 2. An unsteady-state simulation model. *Powder technology*, *99*(1), 46-52.

Sligar, N. J. (1975). *Estimation of Crushing and Classification Functions for and Mathematical Simulation of a Medium Speed Roll/table Mill [manuscript]* (Doctoral dissertation, University of Newcastle).

Svarovsky, L. (2013). *Solid—Gas Separation* (No. 3). Elsevier.

Wei, J. L., Wang, J., & Wu, Q. H. (2007). Development of a multisegment coal mill model using an evolutionary computation technique. *IEEE Transactions on Energy Conversion*, *22*(3), 718-727.

Whiten, W. J., & Özer, C. E. (2015). New relation for the computation of settling velocities and diameters of spheres. *Mineral Processing and Extractive Metallurgy Review*, *36*(2), 92-102.

Zhou, G., Si, J., & Taft, C. W. (2000). Modeling and simulation of CE deep bowl pulverizer. *IEEE Transactions on energy conversion*, *15*(3), 312-322.

Appendix– Mill Model Development

Bowl

Mass balance for coal; the coal feed from feeder tube along with recycle from separator and classifier zones is assumed to drop at the center of the grinding table. Mass balance of coal is given by Eq. (A.1) to (A.2) and the energy balance for the mixing of coal in this section is given by Eq. (A.3)

$$\frac{dM_{ic}^{B}}{dt} = \dot{m}_{ic}^{FB} + \dot{m}_{ic}^{SBa} + \dot{m}_{ic}^{CB} - \frac{M_{ic}^{B}}{\tau_{bg}} \tag{A.1}$$

$$\dot{m}_{ic}^{BG} = \frac{M_{ic}^{B}}{\tau_{bg}} \tag{A.2}$$

$$\begin{aligned} cp_c \frac{d}{dt}\left(T_g \sum (M_{ic}^{B} + M_{ic}^{G})\right) \\ = cp_c\, T_f \dot{m}_{ic}^{FB} + cp_c\, T_{out} \dot{m}_{ic}^{CB} + cp_c\, T_{out} \dot{m}_{ic}^{SB} \\ - cp_c\, T_g \dot{m}_{ic}^{GS} + Q_g \end{aligned} \tag{A.3}$$

Grinding Zone

The Mass balance of coal is represented by Eq (A.4), where the term $\left(-\alpha_i M_{ic}^{G} + \sum_{j=1}^{i} b_{ij} \alpha_j M_{ic}^{G}\right)$ represents the grinding effect. Selection function (α_i) represents the fraction of 'j'th size group that undergoes breakage and is determined using Eq.(A.5). Breakage function (B_{ij}) is used to calculate the elements of breakage matrix (b_{ij}) using Eq. (A.6) to (A.7), where b_{ij} represents the fraction of 'j'th size that is reduced to 'i'th size.

$$\frac{dM_{ic}^{G}}{dt} = \dot{m}_{ic}^{BG} + \left(-\alpha_i M_{ic}^{G} + \sum_{j=1}^{i} b_{ij} \alpha_j M_{ic}^{G}\right) - \dot{m}_{ic}^{GS} \tag{A.4}$$

$$\alpha_i = K_s \, \frac{hg_{coal}}{hg_{ref}} \left(\frac{d_{i,avg}}{d_{ref}}\right)^{0.7} \tag{A.5}$$

$$B_{ij} = \frac{\left[1-\exp\left(\frac{-d_i}{d_j}\right)\right]}{1-\exp(-1)} \quad for\ i\ \geq j,\ \text{Otherwise } B_{ij} = 0 \tag{A.6}$$

$$b_{ij} = B_{i+1\ j} - B_{ij} \quad for\ i\ \geq j,\ \text{Otherwise } b_{ij} = 0 \tag{A.7}$$

The mass balance of moisture in the coal accumulated on grinding table (x^{acc}) is given by Eq. (A.8).

$$\frac{d\left(x^{acc}\sum M_{ic}^{G} + M_{ic}^{B}\right)}{dt} = x^{F}\sum \dot{m}_{ic}{}^{FB} + x^{out}\sum \dot{m}_{ic}^{SB} + x^{out}\sum \dot{m}_{ic}^{CB} - x^{acc}\sum \dot{m}_{ic}^{GS} \tag{A.8}$$

A certain clearance is maintained between the grinder and bowl when the bowl is empty. The force on the coal bed due to the weight of roller can significantly affect the grinding rate and can be adjusted using spring adjustment. The mill power consumption is calculated using an empirical equation as given in Eq. (A.9), where P_{Wo} is the power required to rotate an empty bowl and μ is the frictional coefficient between coal bed and rollers.

$$P_M = \mu\, F\, R\, \omega\, N_{roll} + P_{no\ load} \tag{A.9}$$

$$\mu = C_1\left\{1 - exp\left(-\frac{\sum_{i=1}^{10} M_{ic}^{G}}{C_2}\left(\frac{\sum_{i=8}^{10} M_{ic}^{G}}{\sum_{i=1}^{10} M_{ic}^{G}}\right)^{C_3}\right)\right\} \tag{A.10}$$

Separator Zone

The mass balance of coal in this zone is given by Eq. (A.11) to (A.15), where β represents the fraction of moisture evaporated from coal particles exiting the grinding zone, and separation functions (S_{1i}) determines the fraction of coal passing to the classifier.

$$\frac{dM_{ic}^{S}}{dt} = \dot{m}_{ic}^{GS} - \dot{m}_{ic}^{SC} - \dot{m}_{ic}^{SB} - \dot{m}_{mois,i} \tag{A.11}$$

$$\dot{m}_{ic}^{SB} = (1 - S_{1i})\left(\frac{M_{ic}^{G}}{\tau_{sb}}\right) \tag{A.12}$$

$$\dot{m}_{ic}^{SC} = S_{1i}\left(\frac{M_{ic}^{G}}{\tau_{sc}}\right) \tag{A.13}$$

$$\dot{m}_{mois,i} = \beta_i x^{acc} \dot{m}_{iC}{}^{GS} \tag{A.14}$$

$$\beta_i = 1 - exp\left(\frac{T_{out}}{T_{amb}}\right) \tag{A.15}$$

The separation function is given by Eq. (A.16). The terminal velocity of coal particles passing to classifier is calculated using the average velocity of air in the annular region above the grinding table, as given by Eq.(A.17). Using this average velocity (u_{50}), the cut diameter (d_{50}; in mm) is calculated using a drag force correlation as given in Eq. (A.18) to (A.21).

$$S_{1i} = R_u \exp\left(-0.6931\left(\frac{d_{i,avg}}{d_{50}^{s}}\right)^{\alpha_s}\right) \tag{A.16}$$

$$u_{50} = \frac{4C_e \dot{m}_a}{\rho_a \pi (D_{mt}^2 - D_c^2)} \tag{A.17}$$

$$B = \left(\frac{g\eta_a(\rho_c - \rho_a)}{\rho_a{}^2}\right)^{1/3} \tag{A.18}$$

$$U^* = \frac{u_{50}}{B} \tag{A.19}$$

$$\ln(d^*) = 0.5\,(3.2349\ln(U^*) - 4.591) + [0.25(-2.3311\ln(U^*) + 6.3698)^2 + 5.346]^{0.5} \tag{A.20}$$

$$d_{50}^{s} = \frac{1000\, d^{*} \eta_a}{B \rho_a} \tag{A.21}$$

In this study the geometric dimensions of a ball-race mill (Kojovic et al., 2015) with a similar capacity to IPP mill are presented in Table 1.1**.** The adjustable constant C_e in calculating average air velocity is co-related with the air flow, as given by Eq. (A.22).

$$C_e = 0.0324\dot{m}_a - 0.2483 \tag{A.3}$$

Description	Symbol	Value	Unit
Classifier diameter	D_c	2.38	m
Mill body diameter	D_{mt}	3.14	m

Table 4: Geometric dimensions of the mill used in the calculation of cut diameter (Kojovic et al., 2015)

The mass balance of moisture in this zone is given by Eq. (A.22).

$$\frac{d\left(x^{out} \sum M_{ic}^{S}\right)}{dt} = x^{acc} \sum \dot{m}_{ic}{}^{GS} - x^{out} \sum \dot{m}_{ic}^{SC} + x^{out} \sum \dot{m}_{ic}^{SB} - \sum \dot{m}_{mois,i} \tag{A.4}$$

The energy balance in separator zone is given by Eq.(A.23) to (A.24).

$$\dot{m}_{air} cp_a \left(T_{a,in} - T_{out}\right) = cp_c \left(T_{out} - T_g\right) \sum \left(\dot{m}_{ic}^{SC} + \dot{m}_{ic}^{SB}\right) + h_v \sum \dot{m}_{mois,i} + h_{am}\left(T_{avg} - T_m\right) \tag{A.23}$$

$$M_m cp_m \frac{d}{dt}(T_m) = h_{am}\left(T_{avg} - T_m\right) - h_{me} A_m \left(T_m - T_{amb}\right) \tag{A.24}$$

Classifier Zone

The mass balance of coal in this zone is given by Eq. (A.25) to (A.27), where the separation function (S_{2i}) determines the fraction of coal passing to the furnace.

$$\frac{dM_{ic}^{C}}{dt} = \dot{m}_{ic}^{SC} - \dot{m}_{ic}^{CB} - \dot{m}_{ic}^{CF} \qquad \text{(A.25)}$$

$$\dot{m}_{ic}^{CFu} = \frac{M_{ic}^{C}(S_{2i})}{\tau_{cfu}} \qquad \text{(A.26)}$$

$$\dot{m}_{ic}^{CB} = \frac{M_{ic}^{C}(1 - S_{2i})}{\tau_{cb}} \qquad \text{(A.27)}$$

The separation function based on calculating cut diameter in this zone. For the given cyclone design, a constant Stoke's number corresponding to cut diameter was presented in the study by (Svarovsky, 2013), as given by Eq(A.29).

$$S_{2i} = \exp\left(-0.19\left(\frac{d_{i,avg}}{d_{50}^{c}}\right)^{\alpha_c}\right) \qquad \text{(A.28)}$$

$$stk_{50} = \frac{4\rho_c \dot{m}_a (\, d_{50}^{c})^2}{18\pi\, \rho_a\, \eta_a\, D_c^3} \qquad \text{(A.29)}$$

Product fineness is defined as the fraction of flow passing a 200-mesh screen, as given by Eq.(A.30).

$$Fineness = \frac{\sum_{i=9}^{10} \dot{m}_{ic}^{CFu}}{\sum_{i=1}^{10} \dot{m}_{ic}^{CFu}} \qquad \text{(A.30)}$$

The pressure differential across the mill is given by Eq. (A.31).

$$\Delta P_{mill} = k_a \dot{m}_a^2 + k_{ac} \dot{m}_a^2 \sum_{i=1}^{10} (M_{ic}^G + M_{ic}^B) + k_{en} \dot{m}_a \sum_{i=1}^{10} (M_{ic}^S + M_{ic}^C) \tag{A.31}$$